EUROPEAN JOURNAL OF PURE AND APPLIED MATHEMATICS
2025, Vol. 18, Issue 2, Article Number 5687
ISSN 1307-5543 – ejpam.com
Published by New York Business Global

Existence and Sensitivity Analysis of a Caputo-Fabrizio Fractional Order Vector-Borne Disease Model

Nekmat Ullah[1], Zahir Shah[1,*], Rashid Jan[2,3], S. Islam[4], Narcisa Vrinceanu[5,*], Muhammad Farhan[6], Elisabeta Antonescu[7]

[1] *Department of Mathematical Sciences, University of Lakki Marwat, KPK, Pakistan*
[2] *Department of Mathematics, Saveetha School of Engineering (SIMATS), Thandalam 600124, Chennai, Tamil Nadu, India*
[3] *Institute of Energy Infrastructure (IEI), Department of Civil Engineering, College of Engineering, Universiti Tenaga Nasional (UNITEN), Putrajaya Campus, Jalan IKRAM-UNITEN, 43000 Kajang, Selangor, Malaysia*
[4] *Department of Mechanical Engineering, Prince Mohammad Bin Fahd University, P.O Box 1664, Al Khobar 31952, Saudi Arabia*
[5] *Faculty of Engineering, "Lucian Blaga" University of Sibiu, Romania*
[6] *School of Mathematical Science, Yangzhou University, Yangzhou 225002, China*
[7] *Preclinical Department, Faculty of Medicine, "Lucian Blaga" University, Romania*

Abstract. In this study, we develop a mathematical model for vector-borne infections within a fractional-order framework, employing the Caputo-Fabrizio fractional derivative to enhance the analysis. The steady states of the system are examined, and the basic reproduction number $\mathcal{R}_0$ is derived using the next-generation matrix method. The existence and uniqueness of solutions are established through the application of the Banach fixed-point theorem. A detailed sensitivity analysis of $\mathcal{R}_0$ identifies the most critical parameters influencing the disease dynamics. Numerical simulations are performed to validate the theoretical findings and highlight key factors impacting the control and prevention of the infection. This work provides insights into the dynamics of vector-borne infections and offers a robust mathematical approach for optimizing intervention strategies.

2020 Mathematics Subject Classifications: 92D25, 92D30

Key Words and Phrases: Vector-Borne disease, CF fractional derivative, Mathematical modeling, Existence and uniqueness, Sensitivity analysis, Numerical results

*Corresponding author.
*Corresponding author.
DOI: https://doi.org/10.29020/nybg.ejpam.v18i2.5687

Email addresses: zahir@ulm.edu.pk (Z. Shah), rashid_ash2000@yahoo.com (R. Jan), sislam@pmu.edu.sa (S. Islam), vrinceanu.narcisai@ulbsibiu.ro (N. Vrinceanu)

1. Introduction

Vector-borne diseases are carried through mosquitoes or different kinds of bugs such as houseflies. Vector-borne ailments are mainly studied in vertebrates like mice, rats, nonhuman primates (NHPs), and birds. Investigators want those animals to assist them explore how pathogens are moved from one host to another in addition to determine the feeding behaviors of immune and non-immune individuals as well as selectivity in pathogenicity at different times when hosts feed[1]. The [2] talks about the difficulties encountered when trying to control vector-borne diseases, mainly focusing on mosquitoes as vectors. While there is progress in vaccine technology, challenges such as; resistance of vectors to insecticides, altering ecosystems and the resurgence of some diseases in new regions are still present. The paper states that in order to better handle them, novel surveillance mechanisms, more efficient diagnosis procedures and new ways of controlling such organisms must be put up[3]. The vector-borne diseases explained in [4] indicate how climate change is re-resurfacing or emerging their re-emergence. Moreover, it pointed out that weather elements affect vectors such as mosquitoes hence increasing their numbers resulting into higher chances transmission. Mathematical modeling is a cornerstone of modern biology, enabling researchers to explore complex systems, generate new hypotheses, and design efficient solutions for real-world problems [5–7]. In [8], the researchers focussed on how mathematical models can be used to estimate how much vector-borne viral infections will spread out as well as the speed at which they might go ahead thereby creating an impact. The idea here is that through interventions aimed at lowering R_0 using different approaches one can use such models to control epidemics and pandemic caused by these viruses.

The mathematical model for the dynamics of vector-borne diseases transmitted by mosquitoes is presented in this paper [9], integrating aquatic stages of mosquitoes as well as the gonotrophic cycle. It is illustrated that these elements have an effect on the spread of the disease. Consequently, mosquito-borne illnesses can only be treated efficiently if they aim at these parts. In [10] employs fractional calculus in the representation of malaria transmission with particular reference to impacts of treatment as well as insecticides indicating that disease containment can be optimally achieved through fusion of these techniques using nonlinear ODEs. The fractional-order model with Caputo-Fabrizio derivative is utilized in order to analyze vector-host disease dynamics, such that memory effects (which are important for obtaining better predictions) are emphasized. The paper [11] further provides analytical as well as numerical analyses for exploring on disease behavior including control strategies.In this particular case, a nonlinear fractional-order model was applied in order to take a closer look at vector-borne diseases instead of just using traditional integer-order solid-state models; thus making an improvement through incorporating memory effects. As far as stability goes along with following pathogenesis or epidemiology routes are concerned which leads us to know more about how they can affect each other through time or space[12]. The Caputo-Fabrizio Fractional Order Model which captures the dynamics of COVID-19 pandemic exhibiting greater accuracy than integer-order systems prevalent in past literature by showing improved accuracy when

compared against ordinary models for disease spread within community settings; moreover it illustrates better stability and fits actual/empirical facts as reported by [13].

In [14], the authors utilized a fractional-order Caputo-Fabrizio operator for the modeling of COVID-19 spread; it is shown to provide better descriptions of disease dynamics than those obtained through using integer-order models. It improves comprehension regarding how COVID-19 evolves while facilitating for better policies aimed at curbing its spread. In [15] created a broad similitude model of a fractional-order Boost converter applying the Caputo-Fabrizio principle in governing its system of operation; this has also led to improvement thereof by analysing its effectiveness and possible ways of operation with inductors contained therein.The identification of key parameters influencing cholera's basic reproduction number using sensitivity analysis could assist in the development of intervention strategies that are more effective [16]. The spread of monkeypox in Nigeria in the time of COVID-19 was examined by the researcher in [17], where they estimated the effective reproduction number R_0 during the pandemic.Using mathematical modeling, the basic and effective reproduction numbers of EBOV during the 2014 outbreak in West Africa were estimated as in [18]. In [19] the transmission dynamics of Ebola virus using a Caputo fractional derivative model are examined, thus emphasizing its important parameters like sensitivity for effective control strategies.The article [20] examines issues of the existence of solutions in fractional differential equations, providing a number of basic theorems that underlie these types of problems. The authors employ fixed point theorems to achieve these ends, thereby making a major contribution to the discipline of fractional calculus.

The work in [21] examines how diphtheria spreads in populations by utilizing Caputo fractional derivatives, as it establishes that fixed-point theorems result in solutions which are unique and existent, and in addition carries sensitivity analysis to comprehend the parameters effects towards this model.A fractional-order Caputo operator is used in this study to model the COVID-19 transmission dynamics such that both asymptomatic and symptomatic cases can be effectively captured leading to enhanced accuracy[22]. The article [23] investigates the role of booster vaccination and public enlightenment in tackling infectious diseases using a fractional-order epidemic model (FOEM). The necessity of booster doses and continuous awareness programs in order to successfully curb outbreaks is underscored by the model that shows that even those who have been vaccinated can have the disease. This research delves into the study of that pine wilt disease is transmitted with help from a fractional derivative by Caputo. The main goal of this model is to give insight that the disease can spread across different communities while helping predict what is likely going to happen next as well as coming up with appropriate measures for its containment by using fractional calculus methods that are more efficient in representing memory and hereditary tendencies during its transmission [24]. Caputo derivatives in fractional-order epidemiological models help remember that COVID-19 spreads remotely[25]. The Caputo HIV and Malaria co-infection model applies fractional-order derivatives to appropriately mimic these diseases dynamics and relationships[26]. Investigating rumor spread model dynamics with fractional piecewise derivative[27]. Epidemic models in fractions are a way of using half calculus to explain better how certain diseases, which are contagious spread,

accounting for those times-past effect and difference in population with different hosts [28].

While not all patients receiving antibiotic therapy develop diarrhea, HA CDI is an important and potentially devastating complication in hospitalized patients who require post-treatment follow up and therapy[29]. Since each patient has their own differences, it is a good idea to analyze the individual condition study and find the proper method for each patient. The treatment plan can be tailored best based on the factors [size, type] and recovery time patient is expected to have before suggesting the treatment plan. The effective outcome and fast recovery can be improved with personalized plan of care[30]. Advancing robotics have made surgery more accurate, but because of their prices, which are prohibitively expensive compared to laparoscopy, the future of surgery is these advancements. However, robotic surgery is now being used more often because of its advantages and we know that there are benefits to the practice, such as using ultrasound with contrast agents during inoperative. These have been followed by many novel developed surgical approach allowed surgical outcome to be improved[31]. The factors to consider for selection of the best treatment approach include the physician's experience, patient's characteristics and preference[32].

The importance of fractional epidemic models lies in their ability to generalize traditional approaches, offering greater flexibility in modeling various disease scenarios [33, 34]. In this paper, we present a Caputo-Fabirizo fractional-order VBD model and conduct supplementary qualitative analysis. The effects of parameters associated with R_0 were investigated through sensitivity analyses. This helps identify key elements of the model that should be targeted for effective control strategies. The theoretical results of the vector borne disease model were shown using numerical simulations, which provided information regarding the dynamics. Moreover, we prefer Caputo-Fabrizio derivatives to integer order derivatives as described by CF derivatives because they address real world problems. Specifically, the equilibrium points, R_0, sensitivity as well as its existence and uniqueness are the models under consideration. Section 2 deals with basics preliminaries concept of fractional calculus, In section 3 we formulated CF fractional-order model for VBD and proved the basics results from our derived model. Whereas in section 4 we present the sensitivity analysis. In section 5 we obtain numerical simulation from numerical scheme to look into the impact of various parameters governing the in the dynamics of VBD transmission, and finally, there is the conclusion of our research work.

2. Preliminaries

This section covered some of the most important theoretical ideas related to fractional derivatives, which are necessary for demonstrating the theory analysis of the model.

Definition 1. *[21].The order of the CF fractional derivative* $\alpha\hat{A} \in (0,1)$ *is equivalent to: for the function g(s)*

$$^{CF}D^{\gamma}g(s) = \frac{1}{1-\gamma}\int_0^s g'(\xi)e^{-\frac{\gamma}{1-\gamma}(s-\xi)}\,d\xi. \tag{1}$$

The definition includes a non-singular exponential kernel, which sets it apart from traditional fractional derivatives, and singular kernels are typically found in these definitions.

Definition 2. *A generalized form of the Caputo-Fabrizio Fractional fraction is given as [21]:*

$$c_{\mathbb{D}^p_{0,t}}\psi(t) = \frac{1}{\Gamma(1-p)}\int_0^t \frac{1}{(t-y)^p}\frac{d}{dt}\psi(y)dy, \quad t > 0, \tag{2}$$

is known as the CF derivative of order p of the ψ function. For this, if $p \to 1$, then ${}^E\mathcal{D}^p_{0,t}\psi(t) = \frac{d}{dt}\psi(t)$.

Lemma 1. *[21]. Assuming that $\psi : [0, b] \to \mathbb{R}$ is a continuous and $x \in C^1[0, b]$. Consider*

$$\begin{cases} c_{\mathbb{D}^p_{0,t}}x(t) = \psi(t), t \in [0, b], 0 < p \leq 1, \\ x(0) = x_0, x_0 \in \mathbb{R}. \end{cases} \tag{3}$$

If $x(t)$ satisfies, then $x(t)$ is a solution of the problem (3).

$$x(t) = x_0 + \frac{1}{\Gamma(q)}\int_0^t \psi(y)(t-y)^{p-1}dy.$$

3. Caputo-Fabirizo Fractional VBD Model

The Caputo-Fabrizio fractional-order vector-borne disease (VBD) model is formulated to achieve improved representation of dynamics of vector-host interactions using the Caputo-Fabrizio derivative, which imparts a non-singular kernel and memory effects into the model. This methodology enhances fidelity in representing the disease transmission processes encompassing host and vector populations as opposed to conventional integer-order models[35]. A vector-borne disease transmission model has humans and vectors in its population, where people are classified as susceptible, exposed, infected, and recovered (S_h, E_h, I_h, R_h), while vectors are classified as susceptible, exposed, and infected (S_v, E_v, I_v). The population is susceptible to natural mortality rates, and the model implies that humans who have recovered are immune. The paper analyzes the dynamics of disease propagation with fractional calculus using Caputo-fabirizo derivatives, showing the improved accuracy of fractional-order models. The Caputo-Fabirizo fractional model for VBD is as follow:

$$\begin{cases} \frac{d^\alpha S_h}{du^\alpha} &= \Lambda_h - \beta_1 S_h \frac{I_v}{N_v} - \mu_h S_h, \\ \frac{d^\alpha E_h}{du^\alpha} &= \beta_1 S_h \frac{I_v}{N_v} - (\sigma_h + \mu_h)E_h, \\ \frac{d^\alpha I_h}{du^\alpha} &= \sigma_h E_h - (\gamma + \mu_h)I_h, \\ \frac{d^\alpha R_h}{du^\alpha} &= \gamma I_h - \mu_h R_h, \\ \frac{d^\alpha S_v}{du^\alpha} &= \Lambda_v - \beta_2 S_v \frac{I_h}{N_h} - \mu_v S_v, \\ \frac{d^\alpha E_v}{du^\alpha} &= \beta_2 S_v \frac{I_h}{N_h} - (\sigma_v + \mu_v)E_v, \\ \frac{d^\alpha I_v}{du^\alpha} &= \sigma_v E_v - \mu_v I_v. \end{cases} \tag{4}$$

The definition of its CF derivative operator is as follows:

$$\frac{d^{\alpha}f}{dt^{\alpha}} = \frac{1}{\Gamma(1-\alpha)}\int_0^t (t-s)^{-\alpha} f'(s)\, ds, \tag{5}$$

and $\Gamma(1-\alpha)$ is the gamma function. with I.C:

$$S_h(0) \geq 0, E_h(0) \geq 0, I_h(0) \geq 0, R_h(0) \geq 0, S_v(0) \geq 0, E_v(0) \geq 0, I_v(0) \geq 0.$$

Table 1 explains each state variable and parameter associated with the model (4).

Table 1: Meaning of Variable and Parameter

Variable / Parameter	**Meaning**
$S_h(t)$	Susceptible Population of human
$E_h(t)$	Exposed population of human
$I_h(t)$	Infected population of human
$R_h(t)$	Recovered population of human
$S_v(t)$	Susceptible population of vector
$E_v(t)$	Exposed population of vector
$I_v(t)$	Infected population of vector
α	Fractional derivative order, $0 < \alpha \leq 1$
Λ_h	Birth rate for humans
Λ_v	Birth rate for vectors
β_1	Transmission rate from vectors to humans
β_2	Transmission rate from humans to vectors
σ_h	Progression rate from exposed to infected for humans
σ_v	Progression rate from exposed to infected for vectors
γ	Recovery rate for humans
μ_h	Mortality rate for humans
μ_v	Mortality rate for vectors
N_h	Total human population
N_v	Total vector population

3.1. Analysis of the Caputo-Fabrizio Fractional Model

In this section, we analyze the and existence uniqueness results of the(4) model by using the Banach fixed point theorem. Note that in $\mathcal{Q} = [0, b]$ and sup norm all continuous real value functions and $\mathbb{Y}(\mathcal{Q})$ represent Banach spaces

$$\mathbb{N} = \mathbb{Y}(\mathcal{Q}) \times \mathbb{Y}(\mathcal{Q}) \times \mathbb{Y}(\mathcal{Q}) \times \mathbb{Y}(\mathcal{Q}) \times \mathbb{Y}(\mathcal{Q}) \times \mathbb{Y}(\mathcal{Q}),$$

with norm

$$\|(S_h, E_h, I_h, R_h, S_v, E_v, I_v)\| = \|S_h\| + \|E_h\| + \|I_h\| + \|R_h\| + \|S_v\| + \|E_v\| + \|I_v\|,$$

where

$$\|S_h\| = \max_{u\in\mathcal{Q}} |S_h(u)|, \quad \|E_h\| = \max_{u\in\mathcal{Q}} |E_h(u)|, \quad \|I_h\| = \max_{u\in\mathcal{Q}} |I_h(u)|,$$

$$\|R_h\| = \max_{u\in\mathcal{Q}} |R_h(u)|, \quad \|S_v\| = \max_{u\in\mathcal{Q}} |S_v(u)|, \quad \|E_v\| = \max_{u\in\mathcal{Q}} |E_v(u)|, \quad \|I_v\| = \max_{u\in\mathcal{Q}} |I_v(u)|.$$

For each equation in the(4) system, apply $\mathcal{H}_0^p$ obtained:

$$\begin{cases} S_h(u) &= S_h(0) + \mathcal{H}_0^p[\Lambda_h - \beta_1 S_h \frac{I_v}{N_v} - \mu_h S_h], \\ E_h(u) &= E_h(0) + \mathcal{H}_0^p[\beta_1 S_h \frac{I_v}{N_v} - (\sigma_h + \mu_h) E_h], \\ I_h(u) &= I_h(0) + \mathcal{H}_0^p[\sigma_h E_h - (\gamma + \mu_h) I_h], \\ R_h(u) &= R_h(0) + \mathcal{H}_0^p[\gamma I_h - \mu_h R_h], \\ S_v(u) &= S_v(0) + \mathcal{H}_0^p[\Lambda_v - \beta_2 S_v \frac{I_h}{N_h} - \mu_v S_v], \\ E_v(u) &= E_v(0) + \mathcal{H}_0^p[\beta_2 S_v \frac{I_h}{N_h} - (\sigma_v + \mu_v) E_v], \\ I_v(u) &= I_v(0) + \mathcal{H}_0^p[\sigma_v E_v - \mu_v I_v]. \end{cases} \tag{6}$$

Setting the (6)

$$\begin{cases} \psi_1(u, S_h) &= \Lambda_h - \beta_1 S_h \frac{I_v}{N_v} - \mu_h S_h, \\ \psi_2(u, E_h) &= \beta_1 S_h \frac{I_v}{N_v} - (\sigma_h + \mu_h) E_h, \\ \psi_3(u, I_h) &= \sigma_h E_h - (\gamma + \mu_h) I_h, \\ \psi_4(u, R_h) &= \gamma I_h - \mu_h R_h, \\ \psi_5(u, S_v) &= \Lambda_v - \beta_2 S_v \frac{I_h}{N_h} - \mu_v S_v, \\ \psi_6(u, E_v) &= \beta_2 S_v \frac{I_h}{N_h} - (\sigma_v + \mu_v) E_v, \\ \psi_7(u, I_v) &= \sigma_v E_v - \mu_v I_v. \end{cases} \tag{7}$$

The Lipschitz condition is $\psi_i, i = 1, 2, \ldots, 7$, this implies that there exist an upper bound of $S_h(u), E_h(u), I_h(u), R_h(u), S_v(u), E_v(u)$ and $I_v(u)$. In fact, if we consider two functions, S_h and S_{h1}, such that

$$\begin{aligned} \|\psi_1 - \psi_1\| &= \left\| \left(\beta_1 \frac{\|I_v\|}{N_v} + \mu_h \right) (S_h - S_{h1}) \right\| \\ &\leq \left\| \left(\beta_1 \frac{\|I_v\|}{N_v} + \mu_h \right) (S_h - S_{h1}) \right\|, \end{aligned} \tag{8}$$

$\eta_1 = (\beta_1 n_1 + \mu_h)$, $n_1 = \max_{t\in Q} \frac{\|I_v\|}{N_v}$, where

$$\|\psi_1 - \psi_1\| \leq \eta_1 \|S_h - S_{h1}\|, \tag{9}$$

$0 \leq \eta_1 < 1$ and ψ_1 meet Lipschitz standards. By using the same procedure as before in

(8) and (9), we can get

$$\begin{aligned}
\|\psi_2 - \psi_2\| &\leq \eta_2 \|E_h - E_{h1}\|, \\
\|\psi_3 - \psi_3\| &\leq \eta_3 \|I_h - I_{h1}\|, \\
\|\psi_4 - \psi_4\| &\leq \eta_4 \|R_h - R_{h1}\|, \\
\|\psi_5 - \psi_5\| &\leq \eta_5 \|S_v - S_{v1}\|, \\
\|\psi_6 - \psi_6\| &\leq \eta_6 \|E_v - E_{v1}\|, \\
\|\psi_7 - \psi_7\| &\leq \eta_7 \|I_v - I_{v1}\|.
\end{aligned} \tag{10}$$

In the above (10), we have

$$\eta_2 = \sigma_h + \mu_h, \quad \eta_3 = \gamma + \mu_h, \eta_4 = \mu_h, \quad \eta_5 = (\beta_2 n_5 + \mu_h),$$

$$n_5 = \max_{u \in Q} \frac{\|I_h\|}{N_h}, \eta_6 = \sigma_v + \mu_v, \quad \eta_7 = \mu_v.$$

Thus, system (6) reconstructed the as follows as system (7):

$$\begin{aligned}
S_h(u) - S_h(0) &= \frac{1}{\Gamma(p)} \int_0^u (u-y)^{p-1} \psi_1(y, S_h(u)) dy, \\
E_h(u) - E_h(0) &= \frac{1}{\Gamma(p)} \int_0^u (u-y)^{p-1} \psi_2(y, E_h(u)) dy, \\
I_h(u) - I_h(0) &= \frac{1}{\Gamma(p)} \int_0^u (u-y)^{p-1} \psi_3(y, I_h(u)) dy, \\
R_h(u) - R_h(0) &= \frac{1}{\Gamma(p)} \int_0^u (u-y)^{p-1} \psi_4(y, R_h(u)) dy, \\
S_v(u) - S_v(0) &= \frac{1}{\Gamma(p)} \int_0^u (u-y)^{p-1} \psi_5(y, S_v(u)) dy, \\
E_v(u) - E_v(0) &= \frac{1}{\Gamma(p)} \int_0^u (u-y)^{p-1} \psi_6(y, E_v(u)) dy, \\
I_v(u) - I_v(0) &= \frac{1}{\Gamma(p)} \int_0^u (u-y)^{p-1} \psi_7(y, I_h(u)) dy.
\end{aligned} \tag{11}$$

The recursive form of (11) is as follows:

$$\begin{aligned}
S_{hn}(u) &= \frac{1}{\Gamma(p)}\int_0^u (u-y)^{p-1}\psi_1\left(y, S_{h(n-1)}(u)\right)dy,\\
E_{hn}(u) &= \frac{1}{\Gamma(p)}\int_0^u (u-y)^{p-1}\psi_2\left(y, E_{h(n-1)}(u)\right)dy,\\
I_{hn}(u) &= \frac{1}{\Gamma(p)}\int_0^u (u-y)^{p-1}\psi_3\left(y, I_{h(n-1)}(u)\right)dy,\\
R_{hn}(u) &= \frac{1}{\Gamma(p)}\int_0^u (u-y)^{p-1}\psi_4\left(y, R_{h(n-1)}(u)\right)dy,\\
S_{vn}(u) &= \frac{1}{\Gamma(p)}\int_0^u (u-y)^{p-1}\psi_5\left(y, S_{v(n-1)}(u)\right)dy,\\
E_{vn}(u) &= \frac{1}{\Gamma(p)}\int_0^u (u-y)^{p-1}\psi_6\left(y, E_{v(n-1)}(u)\right)dy,\\
I_{vn}(u) &= \frac{1}{\Gamma(p)}\int_0^u (u-y)^{p-1}\psi_7\left(y, I_{v(n-1)}(u)\right)dy,
\end{aligned} \tag{12}$$

related to $S_{h0} = S_h(0), E_{h0} = E_h(0), I_{h0} = I_h(0), R_{h0} = R_h(0), S_{h0} = S_v(0), E_{h0}$ and $I_{v0} = I_v(0)$. As a result, the difference between concepts that follow produces

$$\begin{aligned}
\Xi_{S_h,n}(u) &= S_{hn}(u) - S_{h(n-1)}(u) = \frac{1}{\Gamma(p)}\int_0^u (u-y)^{p-1}\left(\psi_1(x, S_{h(n-1)}(y)) - \psi_1(y, S_{h(n-2)}(y))\right)dy,\\
\Xi_{E_h,n}(u) &= E_{hn}(u) - E_{h(n-1)}(u) = \frac{1}{\Gamma(p)}\int_0^u (u-y)^{p-1}\left(\psi_2(x, E_{h(n-1)}(y)) - \psi_2(y, E_{h(n-2)}(y))\right)dy,\\
\Xi_{I_h,n}(u) &= I_{hn}(u) - I_{h(n-1)}(u) = \frac{1}{\Gamma(p)}\int_0^u (u-y)^{p-1}\left(\psi_3(x, I_{h(n-1)}(y)) - \psi_3(y, I_{h(n-2)}(y))\right)dy,\\
\Xi_{R_h,n}(u) &= R_{hn}(u) - R_{h(n-1)}(u) = \frac{1}{\Gamma(p)}\int_0^u (u-y)^{p-1}\left(\psi_4(x, R_{h(n-1)}(y)) - \psi_4(y, R_{h(n-2)}(y))\right)dy,\\
\Xi_{S_v,n}(u) &= S_{vn}(u) - S_{v(n-1)}(u) = \frac{1}{\Gamma(p)}\int_0^u (u-y)^{p-1}\left(\psi_5(x, S_{v(n-1)}(y)) - \psi_5(y, S_{v(n-2)}(y))\right)dy,\\
\Xi_{E_v,n}(u) &= E_{vn}(u) - E_{v(n-1)}(u) = \frac{1}{\Gamma(p)}\int_0^u (u-y)^{p-1}\left(\psi_6(x, E_{v(n-1)}(y)) - \psi_6(y, E_{v(n-2)}(y))\right)dy,\\
\Xi_{I_v,n}(u) &= I_{vn}(u) - I_{v(n-1)}(u) = \frac{1}{\Gamma(p)}\int_0^u (u-y)^{p-1}\left(\psi_7(x, I_{v(n-1)}(y)) - \psi_7(y, I_{v(n-2)}(y))\right)dy.
\end{aligned} \tag{13}$$

Assuming That

$$\begin{aligned}
S_{hn}(u) &= \sum_{j=0}^{n} \Xi_{S_{hn},j}(u),\\
E_{hn}(u) &= \sum_{j=0}^{n} \Xi_{E_{hn},j}(u),\\
I_{hn}(u) &= \sum_{j=0}^{n} \Xi_{I_{hn},j}(u),\\
R_{hn}(u) &= \sum_{j=0}^{n} \Xi_{R_{hn},j}(u),\\
S_{vn}(u) &= \sum_{j=0}^{n} \Xi_{S_{vn},j}(u),\\
E_{vn}(u) &= \sum_{j=0}^{n} \Xi_{E_{vn},j}(u),\\
I_{vn}(u) &= \sum_{j=0}^{n} \Xi_{I_{vn},j}(u).
\end{aligned} \tag{14}$$

Thus, based on Equations (9) and (10) as well as the relationships

$$\begin{cases}
\Xi_{S_h,n-1}(u) = S_{h(n-1)}(u) - S_{h(n-2)}(u),\\
\Xi_{E_h,n-1}(u) = E_{h(n-1)}(u) - E_{h(n-2)}(u),\\
\Xi_{I_h,n-1}(u) = I_{h(n-1)}(u) - I_{h(n-2)}(u),\\
\Xi_{R_h,n-1}(u) = R_{h(n-1)}(u) - R_{h(n-2)}(u),\\
\Xi_{S_v,n-1}(u) = S_{v(n-1)}(u) - S_{v(n-2)}(u),\\
\Xi_{E_v,n-1}(u) = E_{v(n-1)}(u) - E_{v(n-2)}(u),\\
\Xi_{I_v,n-1}(u) = I_{v(n-1)}(u) - I_{v(n-2)}(u).
\end{cases} \tag{15}$$

provides

$$\begin{aligned}
\|\Xi_{S_h,n}\| &= \frac{\eta_1}{\Gamma(p)}\int_0^u \|\Xi_{S_h,n-1}\|\,(u-y)^{p-1}dy,\\
\|\Xi_{E_h,n}\| &= \frac{\eta_2}{\Gamma(p)}\int_0^u \|\Xi_{E_h,n-1}\|\,(u-y)^{P-1}dy,\\
\|\Xi_{I_h,n}\| &= \frac{\eta_3}{\Gamma(p)}\int_0^u \|\Xi_{I_h,n-1}\|\,(u-y)^{p-1}dy,\\
\|\Xi_{R_h,n}\| &= \frac{\eta_4}{\Gamma(p)}\int_0^u \|\Xi_{R_h,n-1}\|\,(u-y)^{p-1}dy,\\
\|\Xi_{S_h,n}\| &= \frac{\eta_5}{\Gamma(p)}\int_0^u \|\Xi_{S_v,n-1}\|\,(u-y)^{p-1}dy,\\
\|\Xi_{E_v,n}\| &= \frac{\eta_6}{\Gamma(p)}\int_0^u \|\Xi_{E_v,n-1}\|\,(u-y)^{p-1}dy,\\
\|\Xi_{I_v,n}\| &= \frac{\eta_7}{\Gamma(p)}\int_0^u \|\Xi_{I_v,n-1}\|\,(u-y)^{p-1}dy.
\end{aligned} \tag{16}$$

We construct and prove the subsequent theorem based on the analysis above:

Theorem 1. *Suppose that the function* $\psi_i : [0,T]\times\mathbb{R}^7 \to \mathbb{R}$, *such that* $\psi_i \in D([0,U],\mathbb{R})$ *for any* $S_h(u), E_h(u), I_h(u), R_h(u), S_v(u), E_v(u), I_v(u) \in D([0,T],\mathbb{R})$ *satisfies the Lipschitz and contraction condition* $0 < \eta_i < 1, i = 1,\ldots,7$. *Then, the vector-borne Caputo-fabrizio fractional-order* (4) *possess a unique solution if*

$$\frac{U^p}{\Gamma(p+1)}\eta_i < 1, i = 1,\ldots,7. \tag{17}$$

is true for $t \in [0,U]$.

Remark 1. *Existence and uniqueness results are important in epidemiology, as they need to build mathematical models to predict the spread of diseases and help develop public health policies and vaccination strategies, all of which are necessary to better decision-making. For example, in practical fields such as engineering, physics and biology, the transmission dynamics of COVID-19, HIV/AIDS and disease are just a few examples.*

Proof. The equation (16) provides, if $\psi_i, i = 1,\ldots,7$, meets the Lipchitz condition,

while $S_h(u), E_h(u), I_h(u), R_h(u), S_v(u), E_v(u)$ and $I_v(u)$ are confined.

$$\begin{aligned}
\|\Xi_{S_h,n}(u)\| &\leq \|S_{h0}(u)\| \left(\frac{U^p}{\Gamma(p+1)}\eta_1\right)^n, \\
\|\Xi_{E_h,n}(t)\| &\leq \|E_{h0}(u)\| \left(\frac{U^p}{\Gamma(p+1)}\eta_2\right)^n, \\
\|\Xi_{I_h,n}(tu\| &\leq \|I_{h0}(u)\| \left(\frac{U^p}{\Gamma(p+1)}\eta_3\right)^n, \\
\|\Xi_{R_h,n}(u)\| &\leq \|R_{h0}(u)\| \left(\frac{U^p}{\Gamma(p+1)}\eta_4\right)^n, \\
\|\Xi_{S_v,n}(u)\| &\leq \|S_{v0}(u)\| \left(\frac{U^p}{\Gamma(p+1)}\eta_5\right)^n, \\
\|\Xi_{E_v,n}(u)\| &\leq \|E_{v0}(u)\| \left(\frac{U^p}{\Gamma(p+1)}\eta_6\right)^n, \\
\|\Xi_{I_v,n}(u)\| &\leq \|E_{v0}(u)\| \left(\frac{U^p}{\Gamma(p+1)}\eta_7\right)^n.
\end{aligned} \tag{18}$$

$\Longrightarrow$

$$\begin{aligned}
\|\Xi_{S_h,n}\| &\leq \frac{1}{\Gamma(p)} \int_0^u (u-y)^{p-1} \left(\psi_1\left(y, S_{hn}(y)\right) - \psi_1\left(y, S_{h(n-1)}(y)\right)\right) dy, \\
\|\Xi_{E_h,n}\| &\leq \frac{1}{\Gamma(p)} \int_0^u (u-y)^{p-1} \left(\psi_2\left(y, E_{hn}(y)\right) - \psi_2\left(y, E_{h(n-1)}(y)\right)\right) dy, \\
\|\Xi_{I_h,n}\| &\leq \frac{1}{\Gamma(p)} \int_0^u (u-y)^{p-1} \left(\psi_3\left(y, I_{hn}(y)\right) - \psi_3\left(y, I_{h(n-1)}(y)\right)\right) dy, \\
\|\Xi_{R_h,n}\| &\leq \frac{1}{\Gamma(p)} \int_0^u (u-y)^{p-1} \left(\psi_4\left(y, R_{hn}(y)\right) - \psi_4\left(y, R_{h(n-1)}(y)\right)\right) dy, \\
\|\Xi_{S_v,n}\| &\leq \frac{1}{\Gamma(p)} \int_0^u (u-y)^{p-1} \left(\psi_5\left(y, S_{vn}(y)\right) - \psi_5\left(y, S_{v(n-1)}(y)\right)\right) dy, \\
\|\Xi_{E_v,n}\| &\leq \frac{1}{\Gamma(p)} \int_0^u (u-y)^{p-1} \left(\psi_6\left(y, E_{vn}(y)\right) - \psi_6\left(y, E_{v(n-1)}(y)\right)\right) dy, \\
\|\Xi_{I_v,n}\| &\leq \frac{1}{\Gamma(p)} \int_0^u (u-y)^{p-1} \left(\psi_7\left(y, I_{vn}(y)\right) - \psi_7\left(y, I_{v(n-1)}(y)\right)\right) dy.
\end{aligned} \tag{19}$$

recursively, Using the same procedure, we obtain:

$$\begin{aligned}
\|\Xi_{S_h,n}(u)\| &\leq \|S_{h0}(u)\| \left(\frac{U^p}{\Gamma(p+1)}\eta_1\right)^{n+1}, \\
\|\Xi_{E_h,n}(u)\| &\leq \|E_{h0}(u)\| \left(\frac{U^p}{\Gamma(p+1)}\eta_2\right)^{n+1}, \\
\|\Xi_{I_h,n}(u)\| &\leq \|I_{h0}(u)\| \left(\frac{U^p}{\Gamma(p+1)}\eta_3\right)^{n+1}, \\
\|\Xi_{R_h,n}(u)\| &\leq \|R_{h0}(u)\| \left(\frac{U^p}{\Gamma(p+1)}\eta_4\right)^{n+1}, \\
\|\Xi_{S_v,n}(u)\| &\leq \|S_{v0}(u)\| \left(\frac{U^p}{\Gamma(p+1)}\eta_5\right)^{n+1}, \\
\|\Xi_{E_v,n}(u)\| &\leq \|E_{v0}(u)\| \left(\frac{U^p}{\Gamma(p+1)}\eta_6\right)^{n+1}, \\
\|\Xi_{I_v,n}(u)\| &\leq \|I_{v0}(u)\| \left(\frac{U^p}{\Gamma(p+1)}\eta_1\right)^{n+1},
\end{aligned} \tag{20}$$

to be
$\lim_{n\to\infty} \|\Xi_{S_h,n}(u)\| = 0$, $\lim_{n\to\infty} \|\Xi_{E_h,n}(u)\| = 0$, $\lim_{n\to\infty} \|\Xi_{I_h,n}(u)\| = 0$, $\lim_{n\to\infty} \|\Xi_{R_h,n}(u)\| = 0$, $\lim_{n\to\infty} \|\Xi_{S_v,n}(u)\| = 0$, $\lim_{n\to\infty} \|\Xi_{E_v,n}(u)\| = 0$, $\lim_{n\to\infty} \|\Xi_{I_v,n}(u)\| = 0$.
This ensures that the proposed (4) will have a solution. We follow these steps to prove the uniqueness of the answer. Please allow $S_{h1}(u), E_{h1}(u), I_{h1}(u), R_{h1}(u), S_{v1}(u), E_{v1}(u), I_{v1}(u)$ to be the solution system for (4).

$$\begin{aligned}
\|S_h - S_{h1}\| &= \left\| \frac{1}{\Gamma(p)} \int_0^u (u-y)^{p-1} \psi_1(y, S_h(u)) - \psi_1(y, S_{h1}(u))\, dy \right\|, \\
&\leq \left(\frac{U^p}{\Gamma(p+1)}\eta_1\right) \|S_h - S_{h1}\|.
\end{aligned} \tag{21}$$

Provided that

$$\|S_h - S_{h1}\| \left(1 - \frac{U^p}{\Gamma(p+1)}\eta_1\right) \leq 0. \tag{22}$$

So, $\|S_h - S_{h1}\| = 0$ It's implied.$S_h(u) \to S_{h1}(u)$. We can get $E_h(u), I_h(u), R_h(u), S_v(u), E_v(u)$, and $I_v(u)$ by using the same procedure. This complete the proof of the (1).

The positivity and limit of solutions is an important part of an epidemiological model because of several other features. For this paper, we prove that for every $u > 0$ all state

variables are non-negative. So from system(4) we get:

$$\begin{aligned}
{}^{C}D^{p}_{0,u}S_h(u)\Big|_{S_h=0} &= \Lambda_h \geq 0,\\
{}^{C}D^{p}_{0,u}E_h(u)\Big|_{E_h=0} &= \beta_1 S_h \frac{I_v}{N_v} \geq 0,\\
{}^{C}D^{p}_{0,u}I_h(u)\Big|_{I_h=0} &= \sigma_h E_h \geq 0,\\
{}^{C}D^{p}_{0,u}R_h(u)\Big|_{R_h=0} &= \gamma I_h \geq 0,\\
{}^{C}D^{p}_{0,u}S_v(u)\Big|^{p}_{S_v=0} &= \Lambda_v \geq 0,\\
{}^{C}D^{p}_{0,u}E_v(u)\Big|^{p}_{E_v=0} &= \beta_2 S_v \frac{I_h}{N_h} \geq 0,\\
{}^{C}D^{p}_{0,u}I_v(u)\Big|^{p}_{I_v=0} &= \sigma_v E_v \geq 0.
\end{aligned} \tag{23}$$

Theorem 2. *The region*

$$\Upsilon_h = \left\{(S_h, E_h, I_h, R_h) \in \upsilon_{h+} : 0 < N_h(u) = (S_h(u) + E_h(u) + I_h(u) + R_h(u)) \leq \frac{\Lambda_h}{\mu_h}\right\},$$

and

$$\Upsilon_v = \left\{(S_v, E_v, I_v) \in \upsilon_{v+} : 0 < N_v(u) = (S_v(u) + E_v(u) + I_v(u)) \leq \frac{\Lambda_v}{\mu_v}\right\},$$

are positively invariant for all $u \geq 0$.

Proof. To add the equations of (4) of human and vector compartment, we get

$$\begin{aligned}
{}^{C}D^{p}N_h(u) &= \Lambda_h - \mu_h N_h,\\
{}^{C}D^{p}N_v(u) &= \Lambda_v - \mu_v N_v,
\end{aligned} \tag{24}$$

use of standard comparison theorem [36], provides

$$\begin{aligned}
N_h(u) &\leq \left(N_h(0) - \frac{\Lambda_h}{\mu_h}\right)\mathbb{F}_p\left(-\mu_h t^p\right) + \frac{\Lambda_h}{\mu_h}, \forall u \in [0,\infty),\\
N_v(u) &\leq \left(N_v(0) - \frac{\Lambda_v}{\mu_v}\right)\mathbb{F}_p\left(-\mu_v t^p\right) + \frac{\Lambda_v}{\mu_v}, \forall u \in [0,\infty),
\end{aligned} \tag{25}$$

This implies that $N_h(u) \to \frac{\Lambda_h}{\mu_h}$ $t \to \infty$ and $N_v(u) \to \frac{\Lambda_v}{\mu_v}$ $t \to \infty$.
Next, let $\mathcal{S} = (S_h(u), E_h(u), I_h(u), R_h(u), S_v(u), E_v(u), I_v(u))$, then

$$\Upsilon = \left\{\mathcal{S} \in \mathbb{R}^7_+ : 0 < N_h(u) \leq \frac{\Lambda_h}{\mu_h},\, 0 < N_v(u) \leq \frac{\Lambda_v}{\mu_v}\right\}, \tag{26}$$

is the biologically applicable region of the model (4) of the infection.

3.2. Disease-free Steady State

Here, we denote the disease-free steady state of our system by $\mathcal{E}_0$ and is determined from the following system in the absence of infection:

$$\begin{cases} \Lambda_h - \beta_1 S_h \frac{I_v}{N_v} - \mu_h S_h & = 0, \\ \beta_1 S_h \frac{I_v}{N_v} - (\sigma_h + \mu_h) E_h & = 0, \\ \sigma_h E_h - (\gamma + \mu_h) I_h & = 0, \\ \gamma I_h - \mu_h R_h & = 0, \\ \Lambda_v - \beta_2 S_v \frac{I_h}{N_h} - \mu_v S_v & = 0, \\ \beta_2 S_v \frac{I_h}{N_h} - (\sigma_v + \mu_v) E_v & = 0, \\ \sigma_v E_v - \mu_v I_v & = 0. \end{cases} \tag{27}$$

From the first equation of (27), we have

$$\Lambda_h - \mu_h S_h = 0 \implies S_h^0 = \frac{\Lambda_h}{\mu_h}, \tag{28}$$

and from the fifth equation of (27), we have

$$\Lambda_v - \mu_v S_v = 0 \implies S_v^0 = \frac{\Lambda_v}{\mu_v}. \tag{29}$$

Thus, the DFE of our system is

$$\mathcal{E}_0(S_h^0, E_h^0, I_h^0, R_h^0, S_v^0, E_v^0, I_v^0) = (\frac{\Lambda_h}{\mu_h}, 0, 0, 0, \frac{\Lambda_v}{\mu_v}, 0, 0). \tag{30}$$

3.3. Basic Reproduction Number

The basic reproduction number, $\mathcal{R}_0$, is a key metric in epidemiology, representing the average number of secondary infections caused by one infected individual in a fully susceptible population. It is an important parameter which helps in designing effective control measures, such as vaccination or social distancing, to reduce disease spread.

To calculate $\mathcal{R}_0$, we apply the next-generation matrix method, which includes the matrices $\mathcal{F}$ and $\mathcal{V}$ [17, 18] as

$$F = \begin{pmatrix} 0 & 0 & 0 & \beta_1 \frac{S_h^0}{S_v^0} \\ 0 & 0 & 0 & 0 \\ 0 & \beta_2 \frac{S_v^0}{S_h^0} & 0 & 0 \\ 0 & 0 & 0 & 0 \end{pmatrix}$$

and

$$V = \begin{pmatrix} \sigma_h + \mu_h & 0 & 0 & 0 \\ -\sigma_h & \gamma + \mu_h & 0 & 0 \\ 0 & 0 & \sigma_v + \mu_v & 0 \\ 0 & 0 & -\sigma_v & \mu_v \end{pmatrix}$$

this implies that

$$FV^{-1} = \begin{pmatrix} 0 & 0 & \frac{\beta_1\sigma_v S_h^0}{\mu_v(\mu_v+\sigma_v)S_v^0} & \frac{\beta_1 S_h^0}{\mu_v S_v^0} \\ 0 & 0 & 0 & 0 \\ \frac{\beta_2\sigma_h S_v^0}{(\sigma_h+\mu_h)(\gamma+\mu_h)S_h^0} & \frac{\beta_2 S_v^0}{(\gamma+\mu_h)S_h^0} & 0 & 0 \\ 0 & 0 & 0 & 0 \end{pmatrix} \tag{31}$$

After simplification, $\mathcal{R}_0$ is obtained by

$$\rho\left(\mathcal{F}\mathcal{V}^{-1}\right),$$

as

$$R_0 = \sqrt{\beta_1\beta_2 \frac{\sigma_h\sigma_v}{(\sigma_h+\mu_h)(\gamma+\mu_h)\mu_v(\sigma_v+\mu_v)}} \tag{32}$$

Theorem 3. *The DFE of the model* (4) *is locally asymptotically stable if* $R_0 < 1$*, in any other case it is unstable.*

The endemic equilibrium points of our system is denoted by $\mathcal{E}^*$ and is given by the following

$$\begin{aligned} \mathcal{E}^* &= (S_h^*, E_h^*, I_h^*, R_h^*, S_v^*, E_v^*, I_v^*) \\ &= \left(\frac{\Lambda_h}{\mu_h}\frac{1}{R_0}, \frac{\Lambda_h(R_0-1)\sigma_h+\mu_h}{(\beta_1 N_v+\mu_h\beta_1 S_h^*)\sigma_h}, \frac{\Lambda_h(R_0-1)}{\beta_1\frac{N_v}{I_v}+\mu_h}, \right. \\ &\quad \left. \frac{\gamma\Lambda_h(R_0-1)}{(\beta_1 N_v+\mu_h\beta_1 S_h^*)\mu_h}, \frac{\Lambda_v}{\mu_v}\frac{1}{R_0}, \frac{\mu_v\Lambda_v(R_0-1)}{(\beta_2 N_h+\mu_v\beta_2 S_v^*)\sigma_v}, \frac{\Lambda_v(R_0-1)}{\beta_2\frac{N_h}{I_h}+\mu_v} \right). \end{aligned} \tag{33}$$

4. Sensitivity Index with Respect to $\mathcal{R}_0$

The section below uses a direct sensitivity analysis to determine the significance of specific biological parameters that are linked to the basic reproductive number $\mathcal{R}_0$ in decreasing the spread of vector-borne illnesses [19, 21]:

$$\Pi_\zeta^{R_0} = \frac{\zeta}{R_0} \times \frac{\partial R_0}{\partial \zeta}, \tag{34}$$

is called the sensitivity index of the variable $\zeta \in \{\beta_1, \beta_2\sigma_h, \sigma_v\}, \mu_h, \mu_v, \gamma$, which depends on the value R_0 . To ensure the accuracy of model predictions for parameter values, it is frequently utilized as errors and changes in expected parameters are likely to occur during data collection[21].

In the SEIR model for vector-borne diseases, several key parameters related to disease dynamics are listed in Table 2: β_1 is the human infectious rate with value 0.4, $E_{\beta_1} =$

0.50. The elasticity index indicate that an increase in β_1 increases the number of R_0. β_2 the vector rate of infection having value 0.3, it gives elasticity Value $E_{\beta_2} = 0.50$, it shows that with increase of β_2 the R_0 would be increases.Instead, the human death rate μ_h was set to 0.01 and the vector death rate μ_v was set to 0.05. These parameters have negative elasticities of -0.15 and -0.20, respectively, indicating that the death rate decreases to R_0 because fewer people live in the population and participate in death. The human recovery rate σ_h and the vector recovery rate σ_v are set to 0.5 and 0.4, respectively, and the elasticity indices are 0.08 and 0.10 increase the sensitivity and γ is set 0.1, decrease to -0.42. This means that R_0 decreases with higher recovery rates because survivors no longer die.In general, these parameters and elasticity indices are important for understanding the epidemiology of vector-borne diseases and the effect of various factors on the basic reproduction number R_0. Now below from figure 1: β_1, β_2, Λ_h, and Λ_v, it

Parameter	**Value**	**Elasticity Index**	**Effect**
β_1	0.4	0.50	Increase
β_2	0.3	0.50	Increase
γ	0.1	-0.42	Decrease
μ_h	0.02	-0.17	Decrease
μ_v	0.03	-0.60	Decrease
σ_h	0.2	0.08	Increase
σ_v	0.2	0.10	Increase

Table 2: Parameter values, elasticity indices, and their effects on R_0

follows that increasing these parameters increases $\mathcal{R}_0$ while for parameters μ_h, μ_v, σ_h, and σ_v, increasing these parameters results in a decrease of $\mathcal{R}_0$.

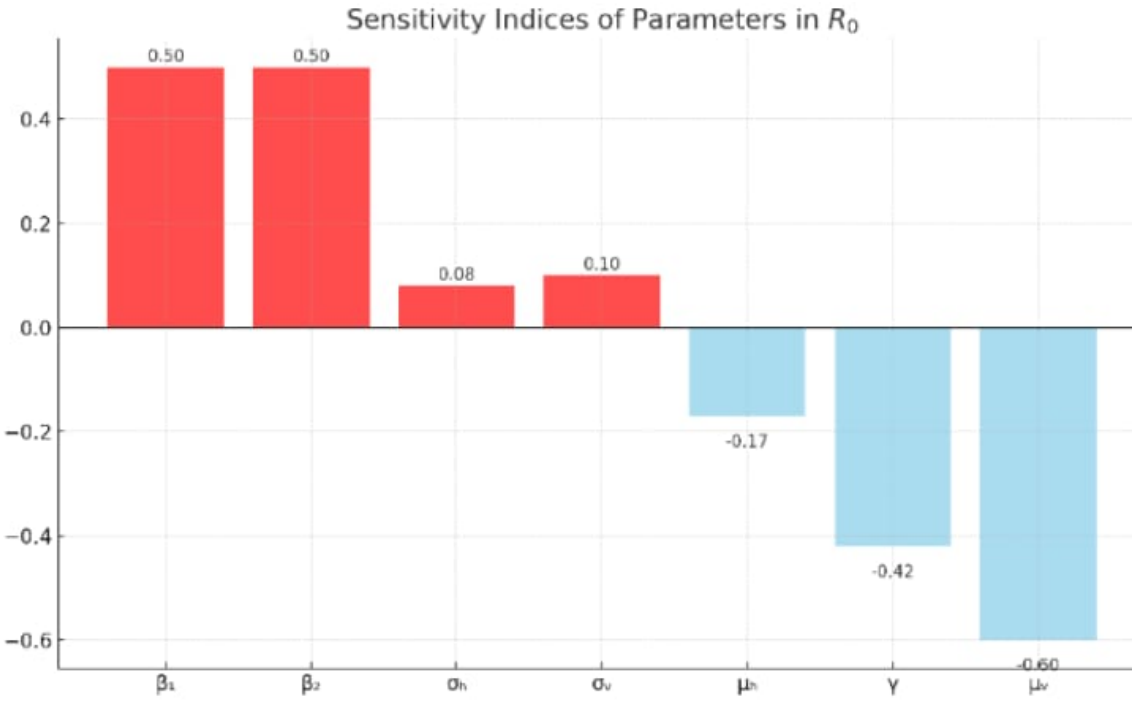

Figure 1: Sensitivity analysis of the basic reproduction number

5. Graphical Analysis and Discussion

To study the dynamic behavior of the model, we may use an efficient numerical model that is stable and convergent, see [24]. The numerical scheme for (4) is as follows:

$$
\begin{aligned}
{}^{\mathrm{C}}S_{h(k+1)} &= b_0 + \frac{r^l}{\Gamma(l+1)} \sum_{m=0}^{k} \Big((k-m+1)^l - (k-m)^l\Big)\,(1-p)(\Lambda_h - (\beta_1 \frac{I_v}{N_v} + \mu_h)S_h) \\
{}^{\mathrm{C}}E_{h(k+1)} &= c_0 + \frac{r^l}{\Gamma(l+1)} \sum_{m=0}^{k} \Big((k-m+1)^l - (k-m)^l\Big)\,(\beta_1 S_h \frac{I_v}{N_v} - (\sigma_h + \mu_h)E_h) \\
{}^{\mathrm{C}}I_{h(k+1)} &= d_0 + \frac{r^l}{\Gamma(l+1)} \sum_{m=0}^{k} \Big((k-m+1)^l - (k-m)^l\Big)\,(\sigma_h E_h - (\gamma + \mu_h)I_h) \\
{}^{\mathrm{C}}R_{h(k+1)} &= e_0 + \frac{r^l}{\Gamma(l+1)} \sum_{m=0}^{k} \Big((k-m+1)^l - (k-m)^l\Big)\,(\gamma I_h - \mu_h R_h) \qquad (35) \\
{}^{\mathrm{C}}S_{v(k+1)} &= f_0 + \frac{r^l}{\Gamma(l+1)} \sum_{m=0}^{k} \Big((k-m+1)^l - (k-m)^l\Big)\,(\Lambda_v - (\beta_2 \frac{I_h}{N_h} + \mu_v)S_v) \\
{}^{\mathrm{C}}E_{v(k+1)} &= g_0 + \frac{r^l}{\Gamma(l+1)} \sum_{m=0}^{k} \Big((k-m+1)^l - (k-m)^l\Big)\,(\beta_2 S_v \frac{I_h}{N_h} - (\sigma_v + \mu_v)E_v) \\
{}^{\mathrm{C}}I_{v(k+1)} &= h_0 + \frac{r^l}{\Gamma(l+1)} \sum_{m=0}^{k} \Big((k-m+1)^l - (k-m)^l\Big)\,(\sigma_v E_v - \mu_v I_v).
\end{aligned}
$$

Understanding the dynamical behavior of an epidemic model is crucial for predicting and

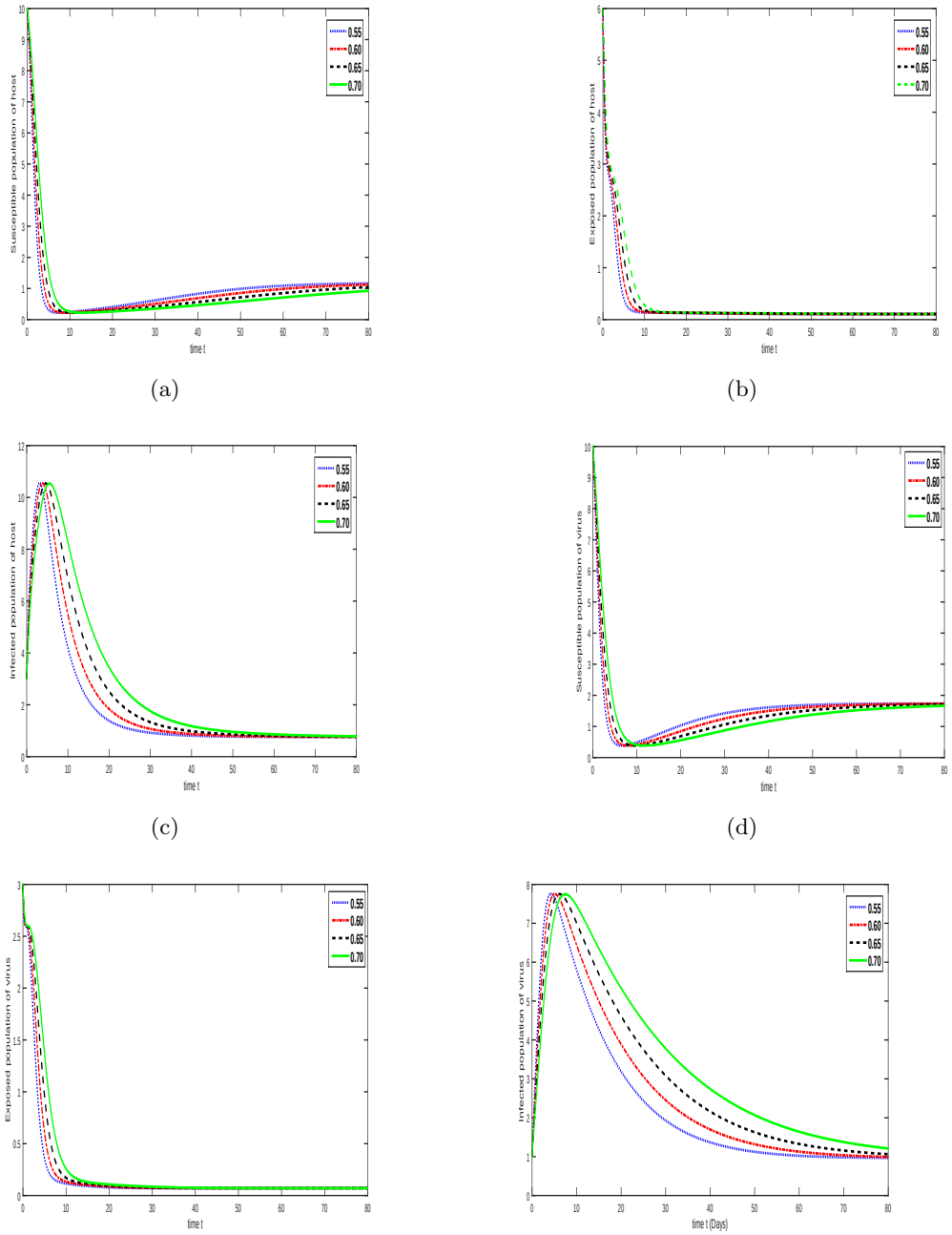

(a) (b)

(c) (d)

(e) (f)

Figure 2: Illustration of human and vector classes for $l = 0.55, 0.6, 0.65, 0.7$.

controlling the spread of infectious diseases. Dynamical behavior refers to how the disease

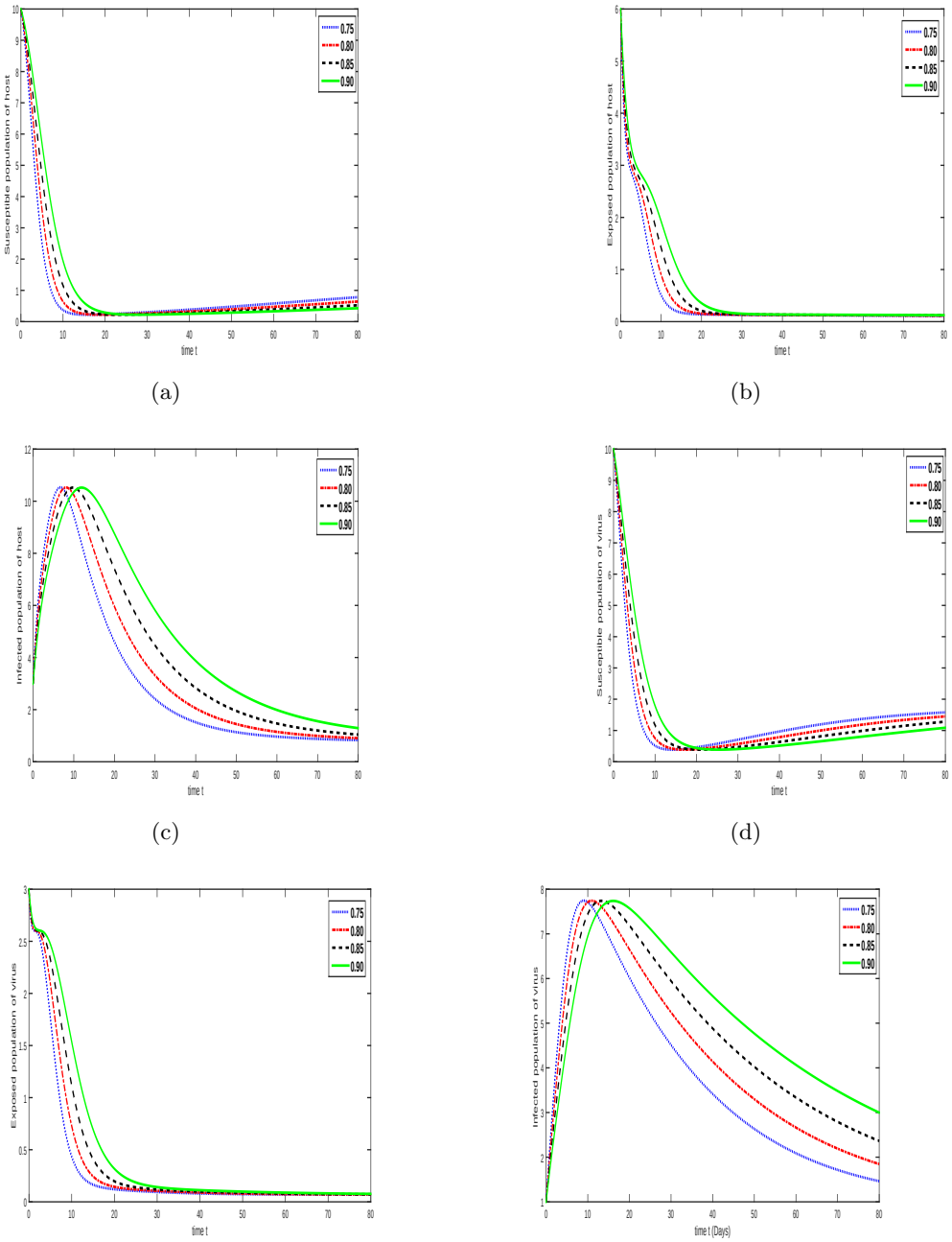

Figure 3: Illustration of human and vector classes for $l = 0.75, 0.8, 0.85, 0.9$.

progresses over time, including the rates of infection, recovery, and mortality, as well as the interplay between susceptible, infected, and recovered populations. This understanding provides a foundation for designing interventions like vaccination campaigns, quarantine

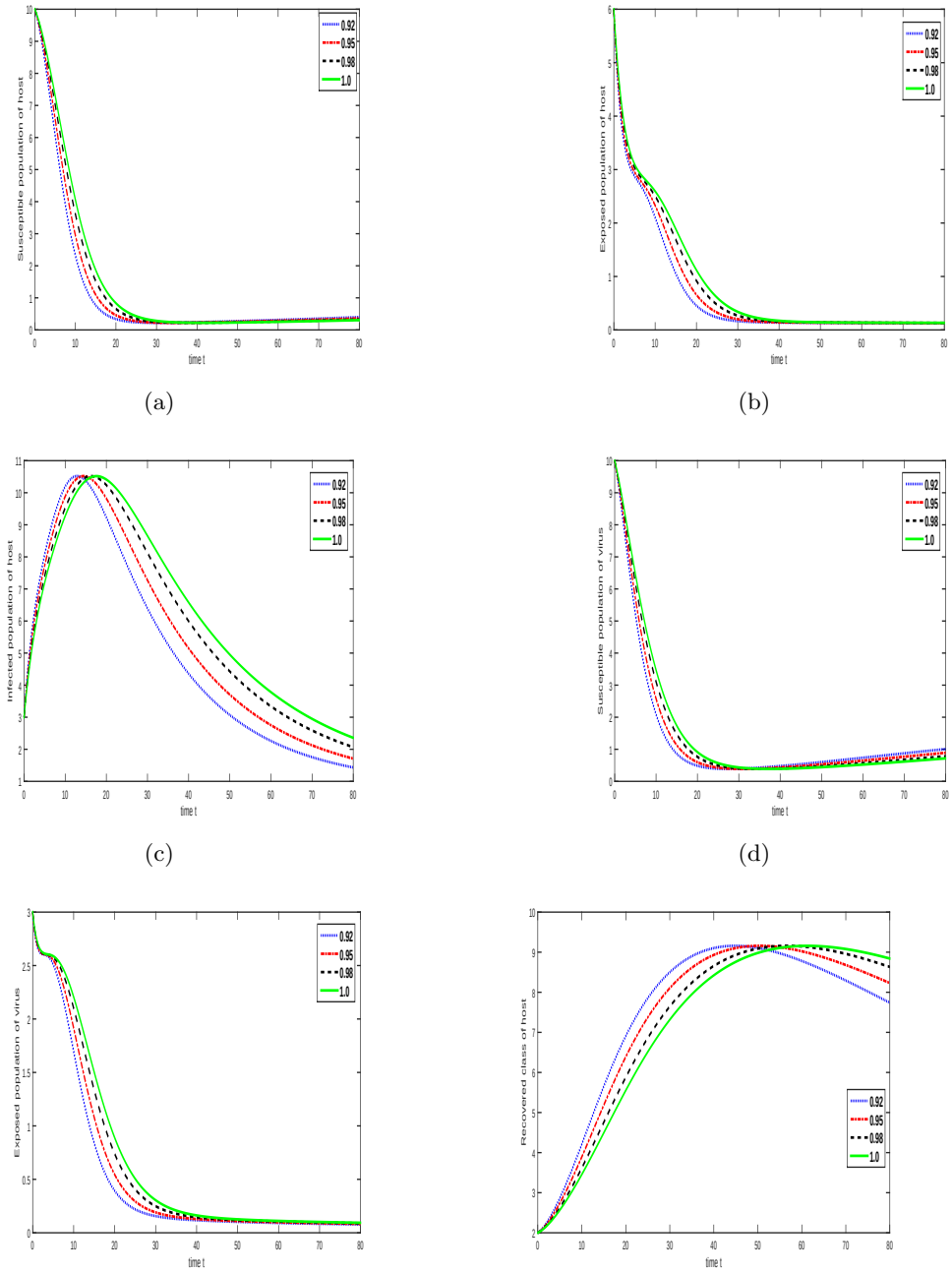

Figure 4: Illustration of human and vector classes for $l = 0.92, 0.95, 0.98, 1$.

measures, or public health policies to mitigate the impact of the disease. Numerical simulations of epidemic models help visualize and evaluate how changes in parameters, such as transmission rates or intervention strategies, affect the course of the outbreak.

For instance, simulations can reveal the timing and magnitude of infection peaks, helping allocate health-care resources effectively. They also allow researchers to assess the long-term outcomes of an epidemic, such as whether the disease will become endemic or be eradicated. Ultimately, studying the dynamical behavior of epidemic models empowers decision-makers to implement timely and effective control measures, reducing morbidity and mortality while minimizing economic and social disruptions.

Here, we perform some simulation to show the impact of fractional parameter on the dynamics of the infection We numerically solved the proposed model (4) and computed the corresponding solutions for both integer and non-integer derivatives, specifically for fractional orders $l = 0.55, 0.6, 0.65, 0.7, 0.75, 0.80, 0.85, 0.9, 0.92, 0.95, 0.98, 1$. The results, as illustrated in Figures 2, 3, and 4, provide insights into the dynamic behavior of the CF fractional-order model. By systematically varying the order fractional order l, we explored the model's intricate dynamics, highlighting deviations from the classical integer-order model. Adjusting the fractional order l revealed significant changes in the population dynamics across different compartments, as visualized in Figures 2, 3, and 4. These adjustments demonstrated an increase or decrease in the number of individuals in each compartment, underscoring the impact of fractional derivatives on the system's behavior. Notably, this approach differs from the classical integer-order model and provides more nuanced control measures. The observed phenomenon offers practical implications for government agencies and medical personnel to better manage and control the spread of infections. Furthermore, our results indicate that as the order l decreases ($0 < l < 1$), the convergence of the system slows, particularly over shorter time scales, emphasizing the sensitivity of the model to fractional dynamics.

6. Conclusions

In this study, a mathematical model for vector-borne infections was developed within a fractional-order framework, utilizing the Caputo-Fabrizio fractional derivative to enhance the analysis. The steady states of the system were examined, and the basic reproduction number $\mathcal{R}_0$ was derived using the next-generation matrix method. The existence and uniqueness of solutions were established through the application of the Banach fixed-point theorem. A detailed sensitivity analysis of $\mathcal{R}_0$ identified the most critical parameters influencing the disease dynamics. Numerical simulations were conducted to validate the theoretical findings and to highlight key factors impacting the control and prevention of the infection. This work provided valuable insights into the dynamics of vector-borne infections and offered a robust mathematical approach for optimizing intervention strategies.

Acknowledgements

Project financed by Lucian Blaga University of Sibiu through the research grant LBUS-IRG-2024.

References

[1] Olayinka M Olajiga, Samuel B Jameson, Brendan H Carter, Dawn M Wesson, Dana Mitzel, and Berlin Londono-Renteria. Artificial feeding systems for vector-borne disease studies. *Biology*, 13(3):188, 2024.

[2] Baldwyn Torto and David P Tchouassi. Grand challenges in vector-borne disease control targeting vectors, 2021.

[3] Daniel Msellemu, Marcel Tanner, Rajpal Yadav, and Sarah J Moore. Occupational exposure to malaria, leishmaniasis and arbovirus vectors in endemic regions: A systematic review. *Current Research in Parasitology & Vector-Borne Diseases*, page 100185, 2024.

[4] Tanvir Hasan, Sadia Afrin, Afroza Sultana, and Ashekul Islam. Asymmetrical reproductive interference between aedes aegypti and aedes albopictus: Implications for coexistence. *Journal of Vector Borne Diseases*, 61(4):547–554, 2024.

[5] Rashid Jan and Asif Jan. Msgdtm for solution of fractional order dengue disease model. *International Journal of Science and Research*, 6(3):1140–1144, 2017.

[6] Wejdan Deebani, Rashid Jan, Zahir Shah, Narcisa Vrinceanu, and Mihaela Racheriu. Modeling the transmission phenomena of water-borne disease with non-singular and non-local kernel. *Computer Methods in Biomechanics and Biomedical Engineering*, 26(11):1294–1307, 2023.

[7] Ahmed Alshehri, Zahir Shah, and Rashid Jan. Mathematical study of the dynamics of lymphatic filariasis infection via fractional-calculus. *The European Physical Journal Plus*, 138(3):1–15, 2023.

[8] Ramakant Prasad, Surendra Kumar Sagar, Shama Parveen, and Ravins Dohare. Mathematical modeling in perspective of vector-borne viral infections: a review. *Beni-Suef University Journal of Basic and Applied Sciences*, 11(1):102, 2022.

[9] Abou Bakari Diabaté, Boureima Sangaré, and Ousmane Koutou. Mathematical modeling of the dynamics of vector-borne diseases transmitted by mosquitoes: taking into account aquatic stages and gonotrophic cycle. *Nonautonomous Dynamical Systems*, 9(1):205–236, 2022.

[10] Muhammad Sinan, Hijaz Ahmad, Zubair Ahmad, Jamel Baili, Saqib Murtaza, MA Aiyashi, and Thongchai Botmart. Fractional mathematical modeling of malaria disease with treatment & insecticides. *Results in Physics*, 34:105220, 2022.

[11] Rashid Jan, Hakima Degaichia, Salah Boulaaras, Ziad Ur Rehman, and Salma Bahramand. Qualitative and quantitative analysis of vector-borne infection through fractional framework. *Discrete and Continuous Dynamical Systems-S*, pages 0–0, 2024.

[12] Pallavi Bedi, Aziz Khan, Anoop Kumar, and Thabet Abdeljawad. Computational study of fractional-order vector borne diseases model. *Fractals*, 30(05):2240149, 2022.

[13] Waleed Adel, Yaser A Amer, Eslam SM Youssef, and Amr MS Mahdy. Mathematical analysis and simulations for a caputo-fabrizio fractional covid-19 model. *Partial Differential Equations in Applied Mathematics*, 8:100558, 2023.

[14] Mati ur Rahman, Saeed Ahmad, RT Matoog, Nawal A Alshehri, and Tahir Khan. Study on the mathematical modelling of covid-19 with caputo-fabrizio operator.

Chaos, Solitons & Fractals, 150:111121, 2021.

[15] Donghui Yu, Xiaozhong Liao, and Yong Wang. Modeling and analysis of caputo–fabrizio definition-based fractional-order boost converter with inductive loads. *Fractal and Fractional*, 8(2):81, 2024.

[16] OJ Peter, AA Ayoade, AI Abioye, AA Victor, and CE Akpan. Sensitivity analysis of the parameters of a cholera model. *Journal of Applied Sciences and Environmental Management*, 22(4):477–481, 2018.

[17] Salihu Sabiu Musa, Zainab Umar Abdullahi, Shi Zhao, Umar Muhammad Bello, Nafiu Hussaini, Abdulrazaq Garba Habib, and Daihai He. Transmission dynamics of monkeypox virus in nigeria during the current covid-19 pandemic and estimation of effective reproduction number. *Vaccines*, 10(12):2153, 2022.

[18] Christian L Althaus. Estimating the reproduction number of ebola virus (ebov) during the 2014 outbreak in west africa. *PLoS currents*, 6, 2014.

[19] Idris Ahmed, Abdullahi Yusuf, Jessada Tariboon, Mubarak Muhammad, Fahd Jarad, and Badamasi Bashir Mikailu. A dynamical and sensitivity analysis of the caputo fractional-order ebola virus model: Implications for control measures. *Science & Technology Asia*, pages 26–37, 2023.

[20] Guotao Wang, Abdeljabbar Ghanmi, Samah Horrigue, and Samar Madian. Existence result and uniqueness for some fractional problem. *Mathematics*, 7(6):516, 2019.

[21] Idris Ahmed, Chanakarn Kiataramkul, Mubarak Muhammad, and Jessada Tariboon. Existence and sensitivity analysis of a caputo fractional-order diphtheria epidemic model. *Mathematics*, 12(13):2033, 2024.

[22] Badr S Alkahtani. Mathematical modeling of covid-19 transmission using a fractional order derivative. *Fractal and Fractional*, 7(1):46, 2022.

[23] Shiv Mangal, OP Misra, and Joydip Dhar. Modeling the effect of vaccination in fractional-order epidemic model for infectious disease. *International Journal of Dynamics and Control*, 12(1):303–317, 2024.

[24] Abdullahi Yusuf, Bahar Acay, Umar Tasiu Mustapha, Mustafa Inc, and Dumitru Baleanu. Mathematical modeling of pine wilt disease with caputo fractional operator. *Chaos, Solitons & Fractals*, 143:110569, 2021.

[25] Isa Abdullahi Baba and Bashir Ahmad Nasidi. Fractional order epidemic model for the dynamics of novel covid-19. *Alexandria Engineering Journal*, 60(1):537–548, 2021.

[26] Idris Ahmed, Abdullahi Yusuf, Musbahu Aminu Sani, Fahd Jarad, Wiyada Kumam, and Phatiphat Thounthong. Analysis of a caputo hiv and malaria co-infection epidemic model. *Thai Journal of Mathematics*, 19(3):897–912, 2021.

[27] Badr Saad T Alkahtani and Sara Salem Alzaid. Studying the dynamics of the rumor spread model with fractional piecewise derivative. *Symmetry*, 15(8):1537, 2023.

[28] Rashid Jan, Muhammad Altaf Khan, Poom Kumam, and Phatiphat Thounthong. Modeling the transmission of dengue infection through fractional derivatives. *Chaos, Solitons & Fractals*, 127:189–216, 2019.

[29] Nicolae Grigore, Maria Totan, Valentin Pirvut, SEBASTIAN IOAN CERNUSCA Mitariu, RADU Chicea, MIHAI Sava, and ADRIAN Hasegan. A risk assessment of clostridium difficile infection after antibiotherapy for urinary tract infections in the

urology department for hospitalized patients. *Rev. Chim*, 68:1453–1456, 2017.

[30] Ionela Mihai, Adrian Boicean, Cosmin Adrian Teodoru, Nicolae Grigore, Gabriela Mariana Iancu, Horatiu Dura, Dan Georgian Bratu, Mihai Dan Roman, Cosmin Ioan Mohor, Samuel Bogdan Todor, et al. Laparoscopic adrenalectomy: tailoring approaches for the optimal resection of adrenal tumors. *Diagnostics*, 13(21):3351, 2023.

[31] Ionela Mihai, Horatiu Dura, Cosmin Adrian Teodoru, Samuel Bogdan Todor, Cristian Ichim, Nicolae Grigore, Cosmin Ioan Mohor, Alin Mihetiu, George Oprinca, Nicolae Bacalbasa, et al. Intraoperative ultrasound: Bridging the gap between laparoscopy and surgical precision during 3d laparoscopic partial nephrectomies. *Diagnostics*, 14(9):942, 2024.

[32] Adrian Ha?egan, Ionela Mihai, Cosmin Adrian Teodoru, Ioana Bogdan Matacuta, Hora?iu Dura, Samuel Bogdan Todor, Cristian Ichim, Denisa Tanasescu, Nicolae Grigore, Ciprian Nicolae Bolca, et al. Exploring the challenges of using minimal invasive surgery to treat stress urinary incontinence: Insights from a retrospective case-control study. *Diagnostics*, 14(3):323, 2024.

[33] Tao-Qian Tang, Rashid Jan, Ziad Ur Rehman, Zahir Shah, Narcisa Vrinceanu, and Mihaela Racheriu. Modeling the dynamics of chronic myelogenous leukemia through fractional-calculus. *Fractals*, 30(10):2240262, 2022.

[34] Sultan Alyobi and Rashid Jan. Qualitative and quantitative analysis of fractional dynamics of infectious diseases with control measures. *Fractal and Fractional*, 7(5):400, 2023.

[35] Jennifer Bravo and Carlos Lizama. The abstract cauchy problem with caputo–fabrizio fractional derivative. *Mathematics*, 10(19):3540, 2022.

[36] Muhammad Farhan, Zahir Shah, Rashid Jan, and Saeed Islam. A fractional modeling approach of buruli ulcer in possum mammals. *Physica Scripta*, 98(6):065219, 2023.